Encapsulation of methylene blue in nucleoside-lipid-based liposomes : physicochemical characterization and evaluation for photodynamic therapy of ovarian cancer

Encapsulation de bleu de méthylène dans des liposomes à base de nucléosides-lipides : caractérisation physicochimique et évaluation pour la thérapie photodynamique du cancer de l'ovaire

KOWOUVI Koffi[1,2*], VERGER Alexis[2,3], GAUBERT Alexandra[4], BARTHÉLÉMY Philippe[4], DOLLO Gilles[2,5], BRANDHONNEUR Nolwenn[2]
[1]Université de Lorraine, CITHEFOR EA3452, Faculté de Pharmacie, Nancy, France.
[2]Univ Rennes, ISCR (Institut des Sciences Chimiques de Rennes) – UMR 6226, F-35000, Rennes, France.
[3]UPR CNRS 4301 CBM, département NMNS, Université de Tours.
[4]Univ. Bordeaux, U1212 INSERM–UMR 5320 CNRS, ARNA, ChemBioPharm, 146 rue Léo Saignat, F-33076 Bordeaux, France.
[5]CHU de Rennes, Pôle Hospitalo-Universitaire de Pharmacie, F-35033 Rennes, France.
(*) Corresponding author: Phone: koffi.kowouvi@univ-lorraine.fr

Reçu le 08 février 2024, accepté le 23 juillet 2024 et publié le 16 septembre 2024

Abstract

Methylene blue liposomes (MB-LPs) intended for photodynamic therapy (PDT) of ovarian cancer were formulated with a negatively charged nucleolipid and phosphatidylcholine using the lipidic film technique followed by an extrusion step. MB-LPs were characterized using dynamic light scattering (DLS), zeta potential (ZP), transmission electron microscopy (TEM), colloidal stability, Fourier-transform infra-red spectroscopy (FT-IR), UV-Visible spectroscopy and cellular studies. MB-LPs were spherical nano-objects with sizes obtained by DLS and TEM between 120 and 130 nm. MB-LPs showed a PDI near 0.10, a negative zeta potential near -42 mV and an encapsulation efficiency around 57 %. Characteristic peaks from ionic interactions of nucleolipids encapsulation of methylene blue were confirmed by FT-IR. Colloidal stability of MB-LPs was slightly affected in complex ionic media, sizes, PDI and ZP remained stable for 4 weeks at all storage temperature tested, allowing a potential use for in vitro and in vivo assays. The use of MB-LPs allowed slightly higher PDT activity based on the production of ROS against SKOV-3 ovarian cancer as compared to MB alone, a reduction of MB dark toxicity and a better protection against oxidation-reduction reactions.

Keywords: methylene blue, nanotechnology, photodynamic therapy, ovarian cancer

Résumé

Des liposomes de bleu de méthylène (BM-LPs), destinés à la thérapie photodynamique (TPD) du cancer de l'ovaire, ont été formulés avec l'association nucléolipide et phosphatidylcholine qui sont chargés négativement. La formulation s'est basée sur la technique d'hydratation de film lipidique suivie d'une étape d'extrusion. Les BM-LPs ont été caractérisés à l'aide de la technique de diffusion dynamique de la lumière (DDL), de détermination du potentiel zêta (PZ), de détermination de la stabilité en milieu colloïdal, de la microscopie électronique à transmission (MET), de la spectroscopie infrarouge à transformée de Fourier (IR-TF), de la spectroscopie UV-Visible et d'études cellulaires. Les BM-LPs sont des nanoparticules sphériques avec des tailles obtenues par DDL et MET entre 120 et 130 nm. Les BM-LPs ont montré un indice de polydispersité IPD proche de 0,10, un potentiel zêta négatif proche de -42 mV et une efficacité d'encapsulation autour de 57 %. Les pics caractéristiques des interactions ioniques entre le bleu de méthylène et les nucléolipides ont été confirmés par IR-TF. La stabilité colloïdale des BM-LPs a été légèrement affectée dans les milieux ioniques complexes, les tailles, IPD et PZ sont restés stables pendant 4 semaines à toutes les températures de stockage testées, permettant une utilisation potentielle pour les essais in vitro et in vivo. L'utilisation de BM-LPs a permis d'obtenir une activité TPD contre le cancer ovarien SKOV-3 légèrement plus élevée, basée sur la production de ROS par rapport à BM seul. Une réduction de la toxicité du BM sans photo-activation et une meilleure protection contre les réactions d'oxydation-réduction ont été observées avec BM-LPs.

Mots-clés : bleu de méthylène, liposomes, thérapie photodynamique, cancer ovarien

1. Introduction

Ovarian cancer is the deadliest gynecological cancer in women [1,2]. In the early phases, the ovarian cancer is mostly asymptomatic, which is why in most cases it is diagnosed at an advanced stage, conferring it a poor prognosis [3,4]. Cytoreductive surgery is the first option for the treatment of ovarian cancer, and chemotherapy alone or combined with surgery is generally used in order to eradicate the non-removable foci [5,6]. Chemotherapy presents various side effects due to the lack of site-specific release, and this can represent a drawback to its usage [7]. Photodynamic therapy (PDT) is a therapeutic approach based on a selective activation of chemical substances called photosensitizers (PS) [8]. This selective activation is based on an absorption of energy from a light source with an appropriate wavelength and power [9]. In this excited form (after absorption), the PS can then present two possible modes of interactions. In the first case (Type I), the PS generates radicals that react directly with O-containing substrates basically by electron transfer and then leads to the production of reactive oxygen species (ROS). In the second case (Type II), the PS can transfer its energy to surrounding oxygen molecules, bringing them to an excited singlet state ($^1O_2$). These reactive species ($^1O_2$ and other ROS) lead to the production of oxygenated free radicals and thus to the tumor destruction [9,10].

PDT can be used in the imaging and treatment of different types of cancer, such as esophageal cancer, prostate cancer, and lung cancer [10]. This can be potentially exploited in the treatment of the ovarian cancer disease, as demonstrated by Brandhonneur et al. [11–13].

A PS needs to follow some specifications: chemical purity, tumor selectivity and minimal dark toxicity with a fast clearance, high photochemical reactivity and activation wavelengths allowing tissue penetration [14,15]. The first-generation of PS (porphyrin, protoporphyrin, uroporphyrin, and hematoporphyrin derivative) partially met these criteria [14], but they had several disadvantages such as a poor selectivity, in terms of target tissue / healthy tissue ratio, low excitation coefficients, relatively short wavelengths for the activation, accumulation in the skin with adverse dermal effects [10,14]. These drawbacks led to the development of second-generation PS, such as phthalocyanine, chlorin, bacteriochlorin, or methylene blue (MB). The latter belongs to the phenothiazine family, and is a positively charged molecule soluble in water and in several organic solvents [16]. MB has several advantages such as an excellent penetration in the cellular membrane, photochemical properties that produce a good quantum yield in the therapeutic window (600-900nm), hydrophilicity, low toxicity and phototoxicity toward a variety of tumor cell lines in-vitro [14,16,17]. Compared to other second-generation PS, MB is low cost and commercially available. It has also high purity, stable composition, and is Food and Drug Administration (FDA) and European Medicines Agency (EMA) approved for therapeutic applications [14,18,19]. One limitation of MB use as PS is its sensitivity to biological environment; reduction in leukomethylene blue (LMB). LMB is an inactivated form with a negligible photodynamic activity [14].

Therefore, MB needs to be integrated into biocompatible delivery systems such as nucleolipid nanocarriers to address these issues with a (i) protection against reduction, (ii) reduction of side effect and toxicity, and (iii) accumulation in cancer cells. Several investigations on the MB encapsulation in matrixes have been done, such as the use of polyacrylamide nanoparticles (NPs), sol-gel silica NPs, organically modified silicate NPs, PLGA NPs, microgel and liposomes (LPs) [9,17,20–23]. The use of nucleolipid-based formulations as potential Drug Delivery System (DDS) has been demonstrated in several studies [24–26].

Very few studies have been conducted to assess MB activity in the treatment of ovarian cancer [27–29] and these studies did not assess activity based on PDT.

The aim of this study was to formulate, characterize and evaluate a novel form of MB liposomes (MB-LPs) with nucleolipid and phosphatidylcholine intended for PDT of ovarian cancer. For this purpose, MB (positively charged molecule), diC16dT (negatively charged nucleolipid), and phosphatidylcholine were used (Fig. 1). MB-LPs were formulated using lipidic film followed by an extrusion step. Negatively charged LPs were obtained by the use of diC16dT [24,30]. MB-LPs were characterized using dynamic light scattering (DLS) (size, polydispersity index), zeta potential, transmission electron microscopy (TEM) (size and shape), colloidal stability over 4 weeks, Fourier-transform infra-red spectroscopy (FT-IR), UV-Visible spectroscopy (encapsulation efficiency and bio-reduction assessment). Free MB and MB-LPs were evaluated with MTT assay (3-(4,5-dimethylthiazol-2-yl)-2,5-diphenyl tetrazolium bromide) for cell cytotoxicity on SKOV-3 ovarian cell. The in vitro generation of ROS was also evaluated by a DCFH-DA method (2',7'-dichlorodihydrofluorescein diacetate).

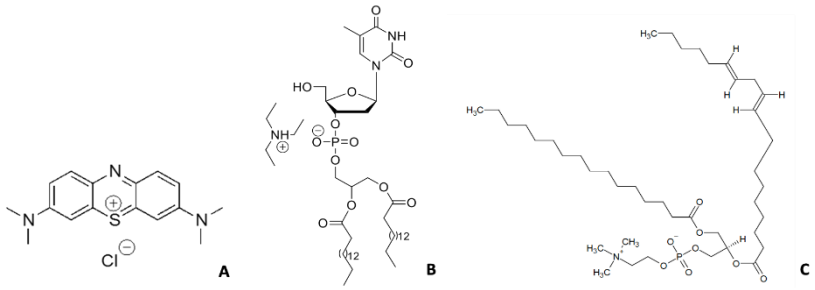

Figure 1 : Chemical structures of methylene blue (A), anionic nucleolipid diC16dT (thymidine 30-(1,2-dipalmitoyl-sn-glycero-3-phosphate)) (B), phosphatidylcholine Lipoid S100 (C)

2. Material and methods

2.1. Chemicals

MB and ascorbic acid were purchased from Cooper (France). diC16dT was synthetized in our laboratory by a Technology Transfer Unit SynVec (Bordeaux, France) according to a published protocole [31]. Phosphatidylcholine (Lipoid S100) was purchased from Lipoid (Ludwigshafen, Germany). 3-(4,5-Dimethylthiazol-2-yl)-2,5-Diphenyltetrazolium Bromide (MTT) and Dimethylsulfoxide (DMSO) were purchased from Sigma Aldrich (St Louis, MO, USA). Dulbecco's Modified Eagle Medium (DMEM) was purchased from Sigma Aldrich (France). Absolute ethanol was purchased from VWR international S.A.S. (Fontenay-sous-bois, France). NaCl was purchased from CDM Lavoisier (France).

2.2. Nanoparticle formulation

507 µL of diC16dT stock solution (4 mg.mL^{-1} in chloroform), 135 µL of Lipoid S100 stock solution (15 mg.mL^{-1} in chloroform), and 5 mL of chloroform were used to obtain a lipidic film after chloroform evaporation under reduced pressure (200 mbar), stirring (150 rpm) at 40°C by a rotary evaporator Laborata 4000 (Heidolph, Schwabach, Germany) for 20 min. The lipidic film was rehydrated using 6 mL of MB stock solution (0.06 mg.mL^{-1} in deionized water) for 30 min under stirring at 150 rpm and at 40°C. A part of deionized water was then removed under reduced pressure (30 mbar), stirring (150 rpm) at 40°C by the rotary evaporator for 10 min and a final volume of 1 mL of suspension was obtained. The obtained product was centrifuged (7000g, 25°C, 2 min) and the supernatant was extruded eleven times (mini-extruder; 100 nm polycarbonate membrane; Avanti Polar Lipids, Alabama, USA) to obtain a nanosuspension of MB-LPs.

2.3. Nanoparticle characterization

2.3.1. **Particles size, polydispersity index and zeta** potential

Particle size, polydispersity index (PDI) and zeta potential (ZP) analyses were determined using a Zetasizer Nano ZS (Malvern Panalytical, Orsay, France). Samples were diluted by 20-fold in deionized water, and measurements were performed at 25°C. Mean diameter and PDI were measured in low volume disposable cuvettes whereas ZP were obtained using folded capillary zeta cells. All analyses were done in triplicate on 3 different batches.

2.3.2. Transmission electron microscopy (TEM)

MB-LPs were characterized by a transmission electron microscope Hitachi H-7650 (Tokyo, Japan). Samples were prepared by loading 6 µL of MB-LPs nanosuspensions onto a carbon-coated copper grid for 3 min before drying. The air-dried samples were then directly examined.

2.3.3. Encapsulation efficiency

Encapsulation efficiency (EE) was determined by UV-Visible spectroscopy. This determination was based on a previous paper [26]. Samples (0.3 mL) were ultra-centrifuged at 40000g for 20 minutes at 20°C. Precipitates were diluted by 20-fold in EtOH and sonicated in an ultrasound bath for 20 minutes. Then the solutions were analyzed in triplicate using a UV-Visible spectrophotometer (Specord®PC 205 UV VIS spectrophotometer, Analytik Jena AG, Jena, Germany). Acquisitions were done in quartz cuvettes with absorbance measurement at 655 nm for quantification.

$$\boldsymbol{EE}\ (\%) = \frac{\textbf{MB in precipitate (mg)}}{\textbf{Total added MB (mg)}}\ \boldsymbol{X}\ \mathbf{100}$$

2.3.4. Fourier transform infrared spectroscopy (FT-IR)

Spectra of Lipoid S100, diC16dt, free MB, blank-LPs and MB-LPs were acquired with a FT-IR spectrometer (FT-IR; VERTEX 70; Bruker). Samples were placed on the ATR module and crushed to ensure a homogeneous distribution on the crystal. All spectra were recorded by averaging 32 accumulations with 4.0 cm^{-1} resolution between 4000 and 400 cm^{-1}.

2.3.5. Stability studies

Colloidal stability in NaCl and DMEM.

To assess MB-LPs stability in in vitro culture medium, a colloidal stability in NaCl and DMEM was performed. MB-LPs were diluted by 20-fold in a NaCl solution (0.9% of NaCl) and in DMEM media. The colloidal stability was assessed based on the size and the PDI.

Colloidal stability at room temperature, 4°C and 37°C.
MB-LPs were stored at room temperature and 4°C for 28 days, and at 37°C for two days. Particle size, PDI and ZP modifications were monitored as previously described in triplicate.
Bio-reduction assessment.
MB-LPs and MB solutions (at the same concentration as MB-LPs) were diluted by 10-fold in deionized water. 100 µL of ascorbic acid solution (100 $mg.mL^{-1}$) was added to 1.9 mL of diluted MB-LPs or MB solutions. Bio-reduction kinetics were monitored at 665 nm for 15 min by a UV-Vis spectrophotometer. The percentage of remaining MB was normalized on initial absorbance. All measurements were done in triplicate.

2.4. Cellular studies

2.4.1. Cell culture

Human ovarian cell carcinoma line SKOV-3 was purchased from Sigma (Sigma Aldrich, France). Cells were cultured in Dulbecco's Modified Eagle Medium (DMEM) and supplemented with 10% fetal bovine serum (FBS) and 1% (v/v) penicillin/streptomycin under a humidified atmosphere (5% CO_2 and 95% air) at 37°C. Cells were cultured in 75 cm^2 Nunclon EasYFlask (Thermo Fisher Scientific, Waltham, USA).

2.4.2. Cellular phototoxicity studies

SKOV-3 cells were seeded into 96-well plates at a density of 20,000 cells/well and cultured for 24h. The cells were then washed with phosphate buffer (PBS) and then freshly prepared MB-LPs were assessed for MB concentration by UV assay and diluted with FBS-free medium, at different concentrations of MB (0.5, 1, 5, 10, 15, 20, 30 and 50 µM). Blank liposomes not loaded with BM were also tested under dilution conditions equivalent to those of BM-loaded liposomes. After administration of the treatments, the cells were incubated for 4 h. The cells were then activated with a light at 660 nm for 10 min to release singlet oxygen and other ROS using a deep-red LED irradiation lamp (Philips, France) with a power of 36W and an irradiance of $40mW/cm^2$. In parallel, a control plate was not activated. Afterwards, cells were re-incubated for a 24h period. Untreated cells (negative control) were considered to have 100% remaining cells and 20 % DMSO treated cells (positive control) were considered to have 0% remaining cells. The cellular cytotoxicity was determined using 3-(4,5-dimethylthiazol-2-yl)-2,5 diphenyltetrazolium bromide (MTT) assay. The tetrazolium ring it contains is reduced to formazan by the mitochondrial succinate dehydrogenase of active living cells. Formazan forms a precipitate in the mitochondria that is proportional to the amount of living cells (but also to the metabolic activity of each cell). MTT was added to cells at concentration of 0.2 $mg.mL^{-1}$ for 3 h, then cell medium was removed and 200 µL DMSO were added to dissolve formazan crystals. For each well, 100 µL of formazan solution was transferred to another 96-well plate and made up to 200 µL using DMSO. Finally, cells cytotoxicity was determined by reading absorbance of formazan at 560 nm using POLARstar Optima microplate reader (BMG labtech, Ortenberg, Germany). Each concentration of MB-LPs was tested in 5 replicates per experiment. All experiments were triplicated on different days.

2.4.3. Semi-quantitative study of ROS production by DCFH-DA assay

To monitor cellular ROS levels, SKOV-3 cells were seeded in 96-well dark plates at a density of 25,000 cells per well. A 24h pre-incubation period allowed the cells to adhere to the bottom of the wells. After washing with PBS, the cells were incubated with 100 mL of a 20 mM solution of DCFH-DA (2',7'-dichlorofluorescein diacetate, Sigma-Aldrich) in PBS for 45 min at 37°C. The cells were then washed with 100 mL of PBS and then incubated with MB and MB-LPs samples at different concentrations of MB in PBS. Blank liposomes not loaded with BM were also tested under dilution conditions equivalent to those of BM-loaded liposomes. After 4h of incubation, a plate was activated at 660 nm for 10 min using a deep-red LED irradiation lamp (Philips, France). Positive controls were treated with 50 mM and 200 mM of hydrogen peroxide. ROS production was measured at 20 min intervals with the POLARstar Optima microplate reader (excitation wavelength: 485 nm, emission wavelength: 520 nm).

2.5. Statistical analysis

Results were expressed as mean values ± standard deviation (SD). A Mann-Whitney test was used for statistical analysis using GraphPad Prism 7.0 software, the level of significance was set at $p < 0.05$. IC_{50} calculation were performed with R software (R foundation, Austria) with the "ic50" package.

3. Results and discussion

3.1. BM-LPs formulation and characterization

MB-LPs were prepared by lipidic film method associated with extrusion. The choice of diC16dT for the lipidic film was based on his negative charge, which is the opposite of the MB charge. This difference between MB charge and the nucleolipid charge increased their interaction [26]. The use of phosphatidylcholine allowed to soften the formed film, because a rigid lipidic film was obtained with phosphatidylcholine-free formulation tests. MB-LPs presented a size of 122.13 ± 5.85 nm by DLS which was confirmed by TEM where particle diameter was around 130 nm, and spherical nano-objects were observed (Fig. 2). MB-LPs size insured the possible use of this DDS by parenteral route [32,33] and the optimal uptake of these particles by tumor cells [34].
MB-LPs showed a PDI of 0.11 ± 0.02 with a negative zeta potential of -41.93 ± 2.37 mV. Blank liposomes (without MB) were also formulated in the same conditions. They showed a size of 125.13 ± 4.06 nm, PDI of 0.06 ± 0.01, and a zeta potential of -57.37 ± 2.70 mV. Both formulations (MB-LPs and blank liposomes) PDI values were under 0.25, indicating that formulations were monodispersed. Zeta potential values were negative due to the diC16dT [24,26], and higher than 30 mV absolute values which is generally related to better nanoparticle physical stabilities due to higher electrostatic repulsion between them [35,36].

The ZP value of blank liposomes was higher than that of MB-LPs. This observation can be explained by the presence of MB (positively charged) on the surface of MB-LPs.
To further explore the organization of the three compounds (MB, diC16dT and Lipoid S100) in the DDS, spectroscopic analyses were performed (Fig. 3). MB (1593 and 1337 cm^{-1} in blue dotted line on the spectrum), diC16dT and Lipoid S100 (2919, 2853, 1691, 1165 and 1121 cm^{-1} for both compound, these bands are shown as green dotted lines on the spectrum) characteristic bands were identified confirming MB-LPs composition, already presented in previous article [26].
The EE was estimated at 57.48 ± 3.60 %, lower than the result obtained by Kowouvi et al. [26] with the formulation of MB nanoparticles by precipitation. This difference may be linked to the addition of phosphatidylcholine (zwitterion molecule) which decreased the MB loading.

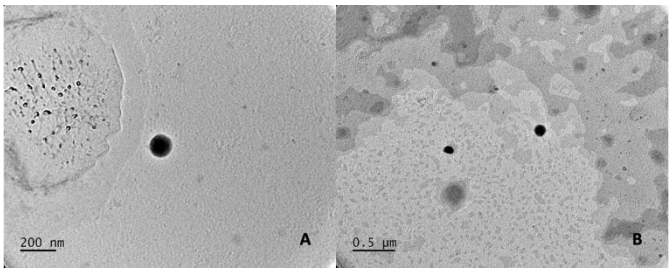

Figure 1: TEM images of MB-LPs.

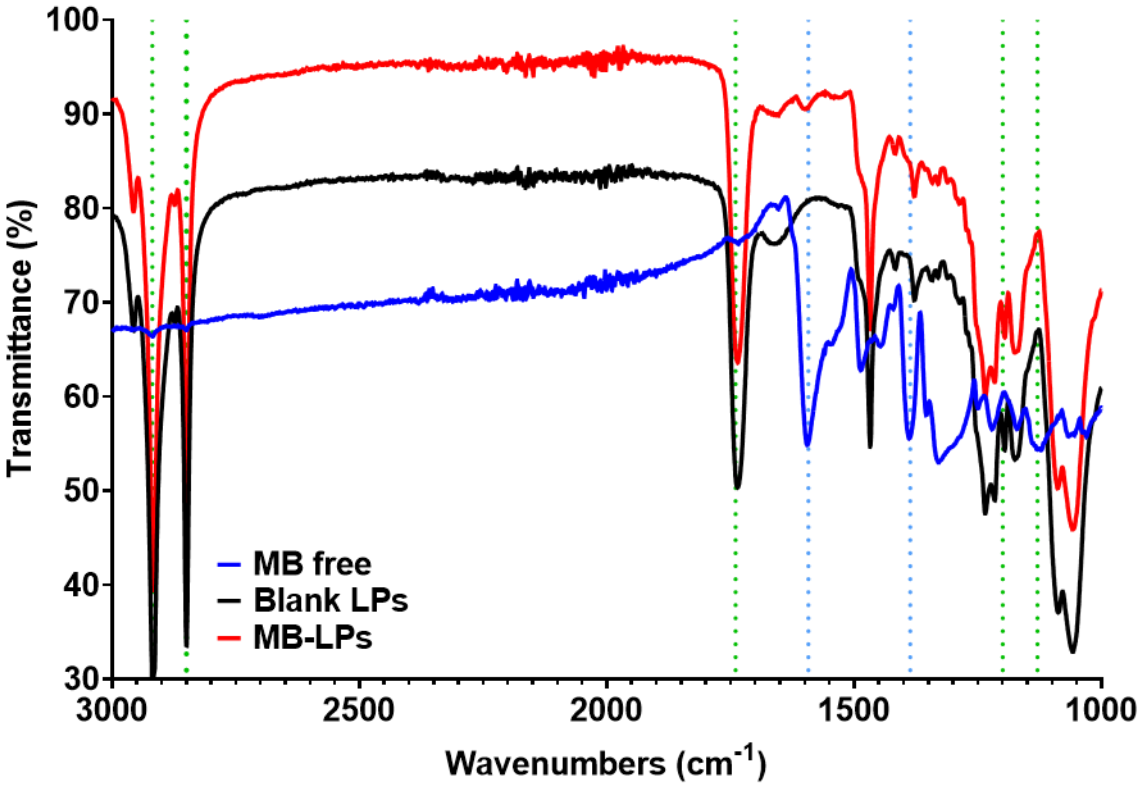

Figure 2: Fourier-transform infrared spectra of free MB (blue), Blank-LPs (black) and MB-LPs (red).

3.2. BM-LPs colloidal stability

The colloidal stability of MB-LPs was assessed in ionic media (NaCl and DMEM) and in different storage conditions (room temperature, 4°C and 37°C).
In ionic media, the dilution of MB-LPs did not affect their size in DMEM (123 ± 9.35 nm), but a slight increase was observed in NaCl (167.67 ± 52.11 nm). In both cases an increase in the PDI was observed but lower than 0.25 (PDI of 0.23 ± 0.08 and 0.22 ± 0.04 in NaCl and DMEM media respectively). Colloidal stability (size, PDI and potential zeta) of MB-LPs was evaluated at room temperature, 4°C and 37°C (Fig. 4). LPs size and PDI remained stable, respectively under 200 nm and 0.3 for all conditions allowing a potential use for *in vitro* and *in vivo* assays (Fig. 4a and 4b). ZP also remained stable for all conditions (Fig. 4c).

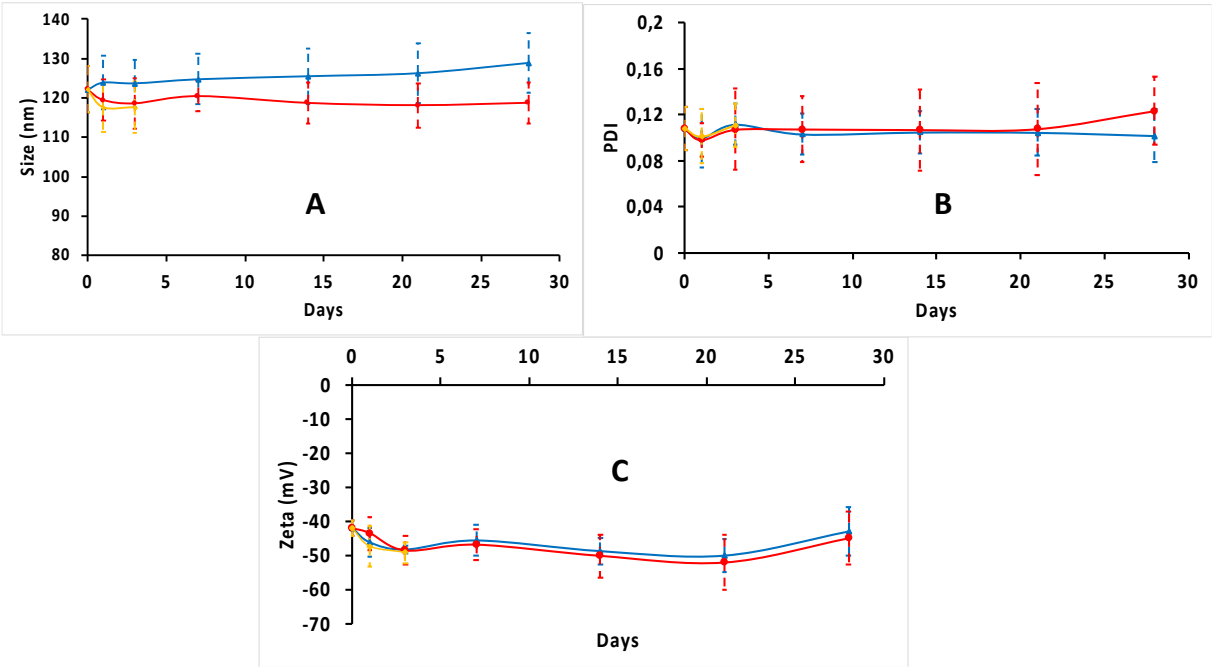

Figure 3: Colloidal stability of MB-LPs over time with particle size (A), PDI (B) and ZP (C) at 37°C (yellow), 4°C (blue) and room temperature (red). Results are the mean ± s.d. of three experiments.

3.3. Bio-reduction assessment

MB is sensitive to oxidation-reduction reactions. The reduced form of MB, known as LMB, is a photo inactive molecule [37]. MB must be protected to have a good PDT activity. This protection can be obtained by its encapsulation. To evaluate the impact of the latter as MB-LPs, a bio-reduction assessment was performed. Ascorbic acid was used as reducing agent and was added to MB and MB-LPs solutions. The reduction kinetics was monitored during 15 min (Fig. 5). The MB reduction was 1.76-fold slower in the case of MB-LPs (24.85 ± 0.63 % preserved) compared to MB solution (8.34 ± 1.68 % preserved). In previous studies a reduction slowdown factor of 1.4 was obtained [26]. This result may be linked to the ionic interaction MB/nucleolipids [26], and the MB loading in the DDS stabilized by phosphatidylcholine [23]. This result also demonstrates the benefit of this new formulation compared to the previous formulation.

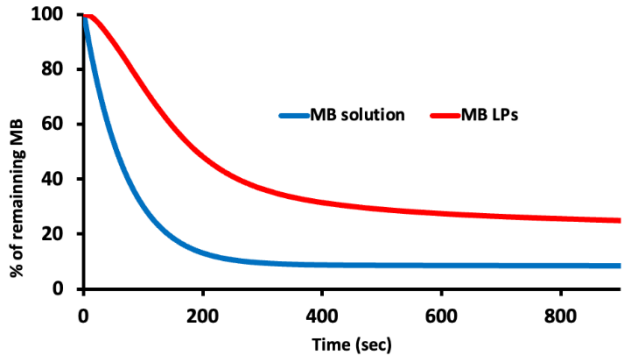

Figure 4: Reduction kinetics of MB solution (blue) and MB-LPs (red) in presence of ascorbic acid based on visible absorption at 665 nm. The widths of the curve represent standard deviation of three independent experiments.

3.4. Cellular phototoxicity studies

The cellular cytotoxicity of SKOV-3 (ovarian cancer cell line) was determined for free MB solution and MB-LPs at several concentrations (0.5–50 µM of MB) to select the concentration of MB-LPs to be used in stimulated conditions. Without UV activation, MB solution was non-toxic for concentrations of 0.5 and 1µM (98.05 and 98.93% respectively; Fig. 6). The cytotoxicity then increased progressively with a calculated IC_{50} of 14.62 ± 1.21 µM. On the other hand, the MB-LPs presented no cytotoxicity up to 20µM (percentage of remaining cells higher than 80%) and a calculated IC_{50} of 48.62 ± 2.10 µM. However, this theoretical value was at the limit of the concentration range used and was considered non-significant. The significant difference between the two calculated IC_{50} (p-value <0.001), confirmed that without light activation, the liposomal formulation was significantly less toxic. In order to evaluate the cellular toxic effect of photo-activation, free MB and MB-LPs were incubated for 4 h (Fig. 7). Even if the theorical IC_{50} were close, 7.72 ± 0.92 µM for the free MB and 6.49 ± 0.47 µM for the MB-LPs, the difference was statistically significant (p-value <0.1), allowing us to conclude on a slight highest efficiency for the liposomal

formulation. MB activity was thus preserved by the liposomal DDS with a slightly increased toxicity by photo-activation and a lowest toxicity without it, decreasing the potential side effects. To find out whether oxidative stress is involved in the biological activity of the compounds, we measured their ability to generate ROS by the fluorometric DFCH-DA. Free MB and MB-LPs at different concentrations were applied. The results showed a significant production of ROS for concentrations of MB (free and encapsulated) between 0,5µM and 50µM (Fig. 8). ROS-induced damage results in cytotoxicity through mitochondrial damage and promotion of apoptotic death [38]. Liposomes not loaded with BM, on the other hand, exhibit no cytotoxicity, maintaining cell viability greater than 80% even at the highest equivalent concentration tested, both with and without UV activation. Additionally, these unloaded liposomes do not generate any reactive oxygen species following UV activation, indicating their stability and safety in cellular environments.

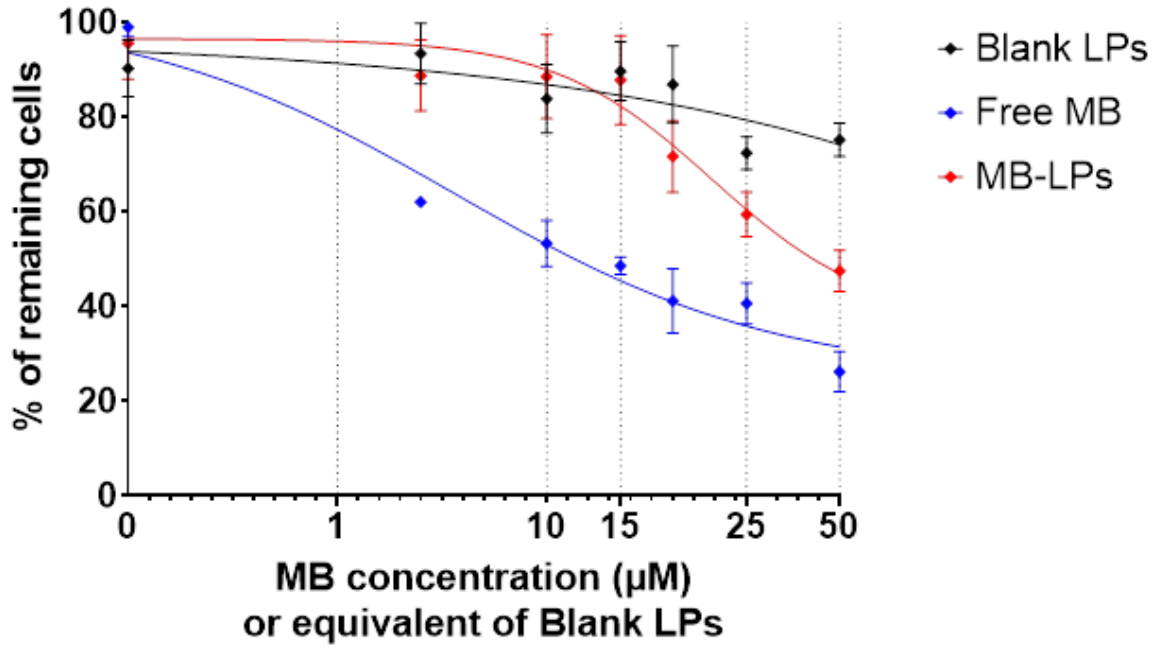

Figure 6: SKOV-3 ovarian cancer cell cytotoxicity after 4h of incubation with Blank LPs (black), MB solution (blue) and MB-LPs (red). Results are the mean ± s.d. of three experiments.

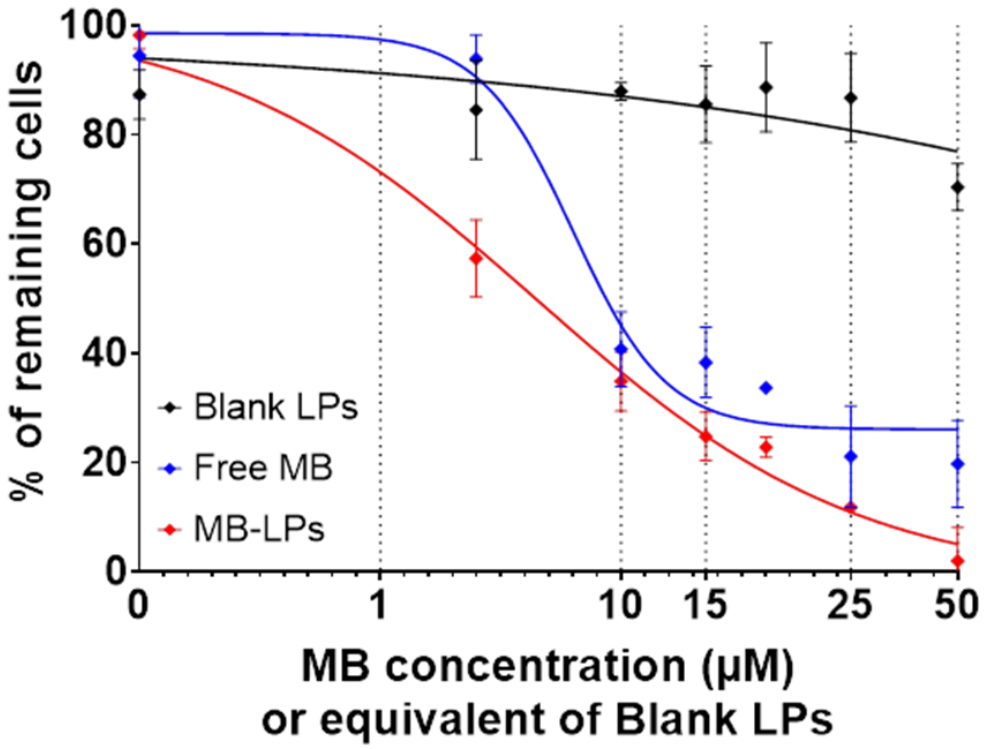

Figure 7: SKOV-3 ovarian cancer cell cytotoxicity after 4h of incubation with Blank LPs (black), MB solution (blue) and MB-LPs (red) with 10 min photoactivation at 660 nm. Results are the mean ± s.d. of three experiments.

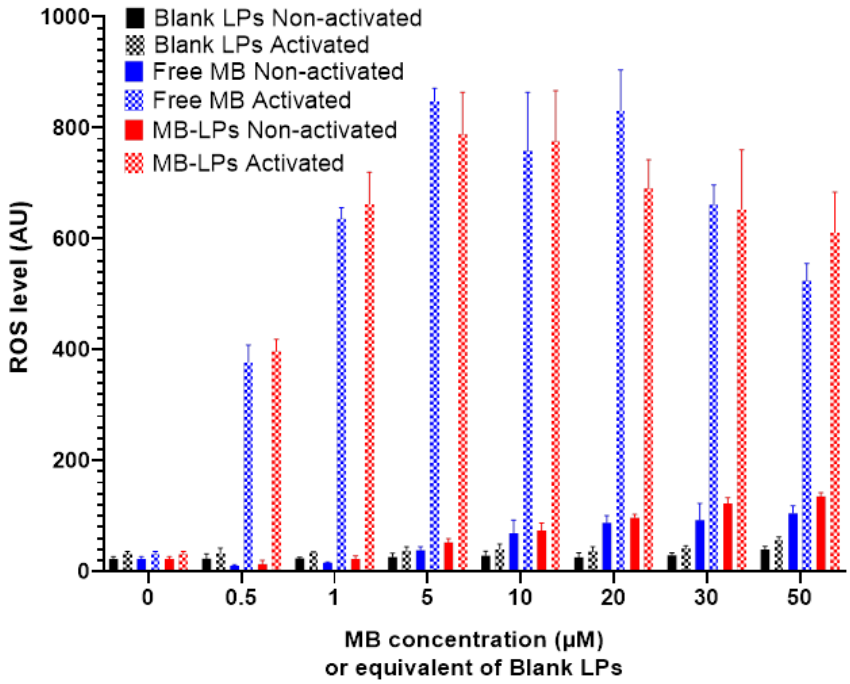

Figure 8: Results for semi-quantitative study of ROS by DCFH-DA with Blank LPs (black), MB solution (blue) and MB-LPs (red), following photoactivation (gridded bars) for 10 min at 660 nm and without photoactivation (full bars).

5. Conclusion

In this study, a novel nanoformulation using MB as PS has been developed. This novel nanoformulation was based on the association of MB with a nucleolipid (diC16dT) and a phosphatidylcholine (Lipoid S100). This assembly led to the formation of stable colloidal liposomes (MB-LPs) even in complex media. The MB encapsulation protected it from redox phenomena due to chemical compounds, ie. ascorbic acid. The study of MB-LPs nanoformulation with a PDT activity against ovarian cancer cell SKOV-3 demonstrated an activity by oxidative mechanism (ROS) and a strong reduction of MB dark toxicity. MB-LPs could be an adjunct to surgery as a surgical dye and as a local PDT agent to lower local and distant recurrence rates. We believe that these findings add a valuable contribution to the investigation of ovarian cancer treatment based on photodynamic therapy.

References

1. Jemal A, Siegel R, Ward E, Hao Y, Xu J, Thun MJ. Cancer statistics, 2009. CA Cancer J Clin. août 2009;59(4):225-49.

2. Ferlay J, Soerjomataram I, Dikshit R, Eser S, Mathers C, Rebelo M, et al. Cancer incidence and mortality worldwide: Sources, methods and major patterns in GLOBOCAN 2012. International Journal of Cancer. 2015;136(5):E359-86.

3. Radu MR, Prădatu A, Duică F, Micu R, Creţoiu SM, Suciu N, et al. Ovarian Cancer: Biomarkers and Targeted Therapy. Biomedicines. 18 juin 2021;9(6):693.

4. Gadducci A, Guarneri V, Peccatori FA, Ronzino G, Scandurra G, Zamagni C, et al. Current strategies for the targeted treatment of high-grade serous epithelial ovarian cancer and relevance of BRCA mutational status. J Ovarian Res. 28 janv 2019;12:9.

5. Kehoe S, Hook J, Nankivell M, Jayson GC, Kitchener H, Lopes T, et al. Primary chemotherapy versus primary surgery for newly diagnosed advanced ovarian cancer (CHORUS): an open-label, randomised, controlled, non-inferiority trial. The Lancet. 18 juill 2015;386(9990):249-57.

6. Rosen B, Laframboise S, Ferguson S, Dodge J, Bernardini M, Murphy J, et al. The impacts of neoadjuvant chemotherapy and of debulking surgery on survival from advanced ovarian cancer. Gynecologic Oncology. 1 sept 2014;134(3):462-7.

7. Markman M. Pharmaceutical management of ovarian cancer : current status. Drugs. 2008;68(6):771-89.

8. Gomes ATPC, Neves MGPMS, Cavaleiro J a. S. Cancer, Photodynamic Therapy and Porphyrin-Type Derivatives. An Acad Bras Ciênc. 2018;90:993-1026.

9. Boccalini G, Conti L, Montis C, Bani D, Bencini A, Berti D, et al. Methylene blue-containing liposomes as new photodynamic anti-bacterial agents. J Mater Chem B. 12 avr 2017;5(15):2788-97.

10. Verger A, Brandhonneur N, Molard Y, Cordier S, Kowouvi K, Amela-Cortes M, et al. From molecules to nanovectors: Current state of the art and applications of photosensitizers in photodynamic therapy. International Journal of Pharmaceutics. 15 juill 2021;604:120763.

11. Brandhonneur N, Boucaud Y, Verger A, Dumait N, Molard Y, Cordier S, et al. Molybdenum cluster loaded PLGA nanoparticles as efficient tools against epithelial ovarian cancer. International Journal of Pharmaceutics. 5 janv 2021;592:120079.

12. Brandhonneur N, Hatahet T, Amela-Cortes M, Molard Y, Cordier S, Dollo G. Molybdenum cluster loaded PLGA nanoparticles: An innovative theranostic approach for the treatment of ovarian cancer. European Journal of Pharmaceutics and Biopharmaceutics. 1 avr 2018;125:95-105.

13. Verger A, Dollo G, Martinais S, Molard Y, Cordier S, Amela-Cortes M, et al. Molybdenum-Iodine Cluster Loaded Polymeric Nanoparticles Allowing a Coupled Therapeutic Action with Low Side Toxicity for Treatment of Ovarian Cancer. Journal of Pharmaceutical Sciences. 1 déc 2022;111(12):3377-83.

14. Tang W, Xu H, Kopelman R, Philbert MA. Photodynamic characterization and in vitro application of methylene blue-containing nanoparticle platforms. Photochem Photobiol. 2005;81(2):242-9.

15. Sivasubramanian M, Chuang YC, Lo LW. Evolution of Nanoparticle-Mediated Photodynamic Therapy: From Superficial to Deep-Seated Cancers. Molecules. 31 janv 2019;24(3):520.

16. Jesus VPS, Raniero L, Lemes GM, Bhattacharjee TT, Caetano Júnior PC, Castilho ML. Nanoparticles of methylene blue enhance photodynamic therapy. Photodiagnosis Photodyn Ther. sept 2018;23:212-7.

17. Tang W, Xu H, Park EJ, Philbert MA, Kopelman R. Encapsulation of Methylene Blue in Polyacrylamide Nanoparticle Platforms Protects its Photodynamic Effectiveness. Biochem Biophys Res Commun. 2 mai 2008;369(2):579-83.

18. Yu J, Hsu CH, Huang CC, Chang PY. Development of therapeutic Au-methylene blue nanoparticles for targeted photodynamic therapy of cervical cancer cells. ACS Appl Mater Interfaces. 14 janv 2015;7(1):432-41.

19. Klosowski EM, de Souza BTL, Mito MS, Constantin RP, Mantovanelli GC, Mewes JM, et al. The photodynamic and direct actions of methylene blue on mitochondrial energy metabolism: A balance of the useful and harmful effects of this photosensitizer. Free Radic Biol Med. juin 2020;153:34-53.

20. Castañeda-Gill JM, Ranjan AP, Vishwanatha JK. Development and Characterization of Methylene Blue Oleate Salt-Loaded Polymeric Nanoparticles and their Potential Application as a Treatment for Glioblastoma. J Nanomed Nanotechnol. août 2017;8(4):449.

21. Khanal A, Bui MPN, Seo SS. Microgel-encapsulated methylene blue for the treatment of breast cancer cells by photodynamic therapy. J Breast Cancer. mars 2014;17(1):18-24.

22. Qin M, Hah HJ, Kim G, Nie G, Lee YEK, Kopelman R. Methylene blue covalently loaded polyacrylamide nanoparticles for enhanced tumor-targeted photodynamic therapy. Photochem Photobiol Sci. mai 2011;10(5):832-41.

23. Wu PT, Lin CL, Lin CW, Chang NC, Tsai WB, Yu J. Methylene-Blue-Encapsulated Liposomes as Photodynamic Therapy Nano Agents for Breast Cancer Cells. Nanomaterials (Basel). 23 déc 2018;9(1):14.

24. Benizri S, Ferey L, Alies B, Mebarek N, Vacher G, Appavoo A, et al. Nucleoside-Lipid-Based Nanocarriers for Sorafenib Delivery. Nanoscale Research Letters. 11 janv 2018;13(1):17.

25. Khiati S, Luvino D, Oumzil K, Chauffert B, Camplo M, Barthélémy P. Nucleoside–Lipid-Based Nanoparticles for Cisplatin Delivery. ACS Nano. 22 nov 2011;5(11):8649-55.

26. Kowouvi K, Alies B, Gendrot M, Gaubert A, Vacher G, Gaudin K, et al. Nucleoside-lipid-based nanocarriers for methylene blue delivery: potential application as anti-malarial drug. RSC Adv. 14 juin 2019;9(33):18844-52.

27. Silva ALG, Carvalho NV, Paterno LG, Moura LD, Filomeno CL, de Paula E, et al. Methylene blue associated with maghemite nanoparticles has antitumor activity in breast and ovarian carcinoma cell lines. Cancer Nanotechnology. 11 mai 2021;12(1):11.

28. Xiang J, Leung AW, Xu C. Effect of Ultrasound Sonication on Clonogenic Survival and Mitochondria of Ovarian Cancer Cells in the Presence of Methylene Blue. Journal of Ultrasound in Medicine. 2014;33(10):1755-61.

29. Xiang J, Xia X, Jiang Y, Leung AW, Wang X, Xu J, et al. Apoptosis of ovarian cancer cells induced by methylene blue-mediated sonodynamic action. Ultrasonics. 1 avr 2011;51(3):390-5.

30. Oumzil K, Ramin MA, Lorenzato C, Hémadou A, Laroche J, Jacobin-Valat MJ, et al. Solid Lipid Nanoparticles for Image-Guided Therapy of Atherosclerosis. Bioconjugate Chem. 16 mars 2016;27(3):569-75.

31. Chabaud P, Camplo M, Payet D, Serin G, Moreau L, Barthélémy P, et al. Cationic Nucleoside Lipids for Gene Delivery. Bioconjugate Chem. 1 mars 2006;17(2):466-72.

32. Aditya NP, Chimote G, Gunalan K, Banerjee R, Patankar S, Madhusudhan B. Curcuminoids-loaded liposomes in combination with arteether protects against Plasmodium berghei infection in mice. Exp Parasitol. juill 2012;131(3):292-9.

33. Nayak AP, Tiyaboonchai W, Patankar S, Madhusudhan B, Souto EB. Curcuminoids-loaded lipid nanoparticles: Novel approach towards malaria treatment. Colloids and Surfaces B: Biointerfaces. 1 nov 2010;81(1):263-73.

34. He C, Hu Y, Yin L, Tang C, Yin C. Effects of particle size and surface charge on cellular uptake and biodistribution of polymeric nanoparticles. Biomaterials. 1 mai 2010;31(13):3657-66.

35. Gupta D, Trivedi P. In vitro and in vivo characterization of pharmaceutical topical nanocarriers containing anticancer drugs for skin cancer treatment. In: Lipid Nanocarriers for Drug Targeting. 2018. p. 563-627.

36. Riddick TM. Control of Colloid Stability Through Zeta Potential: With a Closing Chapter on Its Relationship to Cardiovascular Disease. Zeta-Meter, Incorporated; 1968. 396 p.

37. Hosseinzadeh R, Khorsandi K. Methylene blue, curcumin and ion pairing nanoparticles effects on photodynamic therapy of MDA-MB-231 breast cancer cell. Photodiagnosis Photodyn Ther. juin 2017;18:284-94.

38. Jeng HA, Swanson J. Toxicity of metal oxide nanoparticles in mammalian cells. J Environ Sci Health A Tox Hazard Subst Environ Eng. 2006;41(12):2699-711.